Author Manuscript

Author Manuscript

Author Manuscript

Author Manuscript

HHS Public Access

Author manuscript

Virology. Author manuscript; available in PMC 2016 May 01.

Published in final edited form as:

Virology. 2015 May ; 479-480: 247–258. doi:10.1016/j.virol.2015.02.030.

Development of Animal Models Against Emerging Coronaviruses: From SARS to MERS coronavirus

Troy C Sutton and **Kanta Subbarao**

Laboratory of Infectious Disease, NIAID, NIH

Abstract

Two novel coronaviruses have emerged to cause severe disease in humans. While bats may be the primary reservoir for both viruses, SARS coronavirus (SARS-CoV) likely crossed into humans from civets in China, and MERS coronavirus (MERS-CoV) has been transmitted from camels in the Middle East. Unlike SARS-CoV that resolved within a year, continued introductions of MERS-CoV present an on-going public health threat. Animal models are needed to evaluate countermeasures against emerging viruses. With SARS-CoV, several animal species were permissive to infection. In contrast, most laboratory animals are refractory or only semi-permissive to infection with MERS-CoV. This host-range restriction is largely determined by sequence heterogeneity in the MERS-CoV receptor. We describe animal models developed to study coronaviruses, with a focus on host-range restriction at the level of the viral receptor and discuss approaches to consider in developing a model to evaluate countermeasures against MERS-CoV.

Keywords

coronaviruses; SARS-CoV; MERS-CoV; animal models; receptor

INTRODUCTION

Within the last two decades, there have been several introductions of zoonotic pathogens into the human population. Specifically, two novel coronaviruses (CoV), Severe Acute Respiratory Syndrome-CoV (SARS-CoV) and Middle East Respiratory Syndrome-CoV (MERS-CoV) caused significant concern because they crossed the species barrier and caused severe disease. While SARS-CoV originated in Asia and spread rapidly to several countries throughout the world, MERS-CoV has largely been restricted to infections acquired in the Middle East. Both viruses are associated with spread from person to person and a high case-fatality rate, thus the development of animal models for evaluation of anti-viral therapies and vaccines has been a high priority.

Corresponding author: Kanta Subbarao, Phone: 301-451-3839, ksubbarao@niaid.nih.gov.

Publisher's Disclaimer: This is a PDF file of an unedited manuscript that has been accepted for publication. As a service to our customers we are providing this early version of the manuscript. The manuscript will undergo copyediting, typesetting, and review of the resulting proof before it is published in its final citable form. Please note that during the production process errors may be discovered which could affect the content, and all legal disclaimers that apply to the journal pertain.

Author Manuscript Author Manuscript Author Manuscript Author Manuscript

SARS-CoV emerged in the Guangdong province of southern China in November, 2002 (1). Retrospective analysis identified 11 cases between November 2002 and March 2003. Of these, 7 had documented contact with wild animals (2–4). In February, 2003 an infected person travelled to Hong Kong and stayed at Hotel M (5). At the hotel, he spread the virus to several visitors who returned to their home countries (Canada, Ireland, the United States, Vietnam and Singapore) starting the global SARS-CoV epidemic (4–8). In total, 8437 SARS-CoV cases with 813 fatalities were reported (9, 10). As a result of a coordinated public health effort involving screening, isolation, contact tracing and quarantine efforts, the human chain of transmission of SARS-CoV was broken (9, 11–14). Since the end of the outbreak, there have been a few incidents of laboratory-acquired SARS-CoV infections (15–17), and over two weeks in December 2003 to January 2004, 4 individuals in Guangzhou, China became infected with SARS-CoV. None of these patients died from infection and the virus was not transmitted to contacts (17). Since early 2004, SARS-CoV has not re-emerged and no new community-acquired infections have been reported. However, closely related coronaviruses have been identified in bats and at least one bat virus is able to bind the human receptor and infect human cells (18, 19).

In contrast, the MERS-CoV outbreak is on-going. MERS-CoV was initially isolated from a severely ill patient in Jeddah, Saudi Arabia, in June of 2012 (20, 21). Since then, there have been continued reports of new infections in geographically distinct regions suggesting separate zoonotic introductions (22). Secondary transmission to health-care workers and family members has also been reported, and the WHO estimates that up to 75% of cases represent secondary infections (23). As of early December 2014, 955 laboratory confirmed cases of MERS-CoV infection and 386 deaths have been reported (24). MERS-CoV infections have been reported in at least 9 countries in the Middle East including Saudi Arabia, United Arab Emirates (UAE), Qatar, Oman, Jordan, Kuwait, Yemen, Lebanon, and Iran, and there have been isolated incidents of infected travellers returning to countries in Europe, South East Asia, and the United States (25–34).

Both SARS-CoV and MERS-CoV belong to the order *Nidovirales*, family *Coronavirus*. They are both betacoronaviruses and belong to lineages B and C, respectively (1, 19, 20). As members of the Coronaviridae family, both viruses have a host cell derived lipid envelope and contain a non-segmented positive-stranded RNA genome (35, 36). The viral genome encodes a series of nested subgenomic RNAs that express multiple gene products. Coronaviruses attach and enter cells via interactions of the Spike (S) protein with cell surface receptors. For SARS-CoV, human Angiotensin-converting enzyme 2 (ACE2) and CD209L were identified as cellular receptors (37, 38); ACE2 is the predominant receptor as CD209L has a much lower affinity for the S protein (38). The cell surface receptor for MERS-CoV is human dipeptidy peptidase 4 (hDPP4), also known as CD26 (39). For both SARS and MERS-CoV, the S protein host-receptor interaction is considered a major determinant of host restriction (35).

Both viruses are closely related to coronaviruses identified in bats: bat-SARS-CoV from Chinese horseshoe bats and SARS-CoV (19), and HKU4, HKU5 and MERS-CoV (19, 20). While bats may be the primary reservoir for MERS-CoV, surveillance studies found high rates of seropositivity in dromedary camels from several Middle Eastern countries (25–30)

Author Manuscript Author Manuscript Author Manuscript Author Manuscript

indicating that camels play a role as a reservoir. This was strengthened by studies that identified MERS-CoV RNA in nasal swabs from 3 camels on a farm associated with 2 human cases (31), and additional studies in which a camel isolate was directly linked to a fatal human case in Saudi Arabia (32, 33). Furthermore, experimental infection of dromedary camels demonstrated that they could be productively infected and shed high titers of virus in their nasal secretions (34). However, the relative role of camels and bats as reservoirs for MERS-CoV remains to be determined.

For SARS-CoV, several animal species were evaluated as models of human disease and while most laboratory animals including mice, hamsters, ferrets and non-human primates could be productively infected (40), few species displayed overt clinical disease. Following serial adaptation of SARS-CoV in mice (41) and the engineering of transgenic mice to express human ACE2 (42, 43), this obstacle was partially overcome. The development of these murine models enabled efficacy studies of anti-viral agents and several vaccines against SARS-CoV (44, 45). In contrast, several animal species have been evaluated for MERS-CoV but with the exception of some primate species, most animals are resistant to infection. Herein, we describe the animal models for both SARS and MERS-CoV with a focus on the role of the host receptor. We conclude by discussing other approaches that could be used to develop animal models of MERS-CoV.

Strategies for the Development of Animal Models of Infectious Diseases

Animal models of infectious diseases serve two key purposes: 1) to characterize viral pathogenesis, and 2) to evaluate anti-viral agents and vaccines. In the context of infectious diseases for which it is not feasible or ethical to perform clinical trials, animal studies play an additional role. Under the FDA's *Animal Efficacy Rule* ("Animal Rule") therapeutics against rare, emerging, or virulent agents can achieve regulatory approval provided efficacy is demonstrated in two animal models (one of which must be a non-rodent species) that display clinical illness representative of human disease (46).

The ideal animal model is permissive to infection and reproduces the clinical course and pathology observed in humans. An algorithm for the development of animal models is presented in Figure 1. Small animal models offer several advantages over NHP's including availability of animals and species specific reagents, ease of handling, reduced cost, and the ability to use sufficient numbers for statistical analysis. Especially with coronaviruses, rodents vary in susceptibility and may be semi-permissive to infection and refractory to clinical disease (47), even so, they can be used to screen countermeasures (48–51). Thus, to generate a rodent model that displays clinical disease it may be necessary to adapt the virus to enhance virulence for the rodent host or generate transgenic animals. Pathogenesis in these models should be fully characterized because the disease mechanism of an adapted virus or in a transgenic animal may be different from that in the natural host (Figure 1).

As NHPs are closely related to humans, they are invaluable as animal models. Since studies in NHP incur significant expense, most investigators choose to screen therapies in small animal models and then perform more limited primate studies. It is important to note that there are several species and subspecies of NHP that can result in significant variation in the

Author Manuscript Author Manuscript Author Manuscript Author Manuscript

level of viral replication and clinical disease. Thus, several species must often be evaluated to yield a suitable animal model. Collectively, the development of animal models in both rodents and NHP has been fundamental to the study of infectious diseases and has lead to the development of countermeasures against several zoonotic pathogens.

Animal Models of SARS-CoV

Mouse Models

Several inbred mouse strains have been evaluated as models for SARS-CoV infection (47, 52–54). Initial studies in 4–6 week old BALB/c mice demonstrated that virus doses of 10^3 and 10^5 median tissue culture infectious doses ($TCID_{50}$) of the Urbani strain given intranasally resulted in a productive infection with peak titers on day 3 and resolution by day 7. Mice did not lose weight, display signs of clinical disease or develop pulmonary pathology. Studies in C57BL/6 (B6) mice yielded similar results, with a lack of clinical disease and clearance of virus by day 9. Knockout mice on the B6 background including beige and $CD1^{-/-}$ strains that lack NK cell function and NK-T cells, respectively, and $RAG1^{-/-}$ mice that lack T and B lymphocytes also did not develop clinical disease. Viral kinetics were similar in B6, beige, $CD1^{-/-}$ mice, and $RAG1^{-/-}$ mice (52). Similarly, 129SvEv mice displayed peak viral replication on day 3 with clearance by day 8 and did not develop clinical illness. Histopathological examination showed evidence of self-limiting bronchiolitis and patchy interstitial pneumonia. In contrast, disease progression was significantly altered in $STAT1^{-/-}$ mice on the 129SvEv background. $STAT1^{-/-}$ mice displayed progressive weight loss and bronchiolitis that progressed to interstitial pneumonia and mediastinitis (53). Viral replication peaked on day 3 and persisted until day 22 post-infection indicating that a type I IFN response is required to control SARS-CoV infection. Although mice showed evidence of infection and lung disease, inbred mouse strains did not accurately reproduce the diffuse alveolar damage, edema, pneumocyte necrosis, and hyaline membrane formation observed in humans (55–57).

To model the epidemiological finding that advanced age resulted in increased mortality, an aged mouse model of SARS-CoV was developed. In this model, 12–14 month old BALB/c and B6 mice support high levels of viral replication in the lungs from day 2 to 6 with resolution by day 9. Both strains of mice lose weight (~7–8% on day 5) and aged BALB/c mice displayed ruffled fur and dehydration (40, 58). In contrast, aged 129SvEv mice did not support prolonged pulmonary viral replication and cleared the virus by day 5 (40). Regardless, all aged mouse strains displayed similar histopathological features early during infection (i.e. day 3) including perivascular and peribronchiolar mononuclear infiltrates, necrotic debris in the bronchioles, and foci of interstitial pneumonitis (40, 58). On day 5 post-infection, aged BALB/c mice displayed prominent perivascular infiltrates and alveolar damage that persisted until day 9 (58). Collectively, the pathological changes observed in the aged mouse model more closely resemble those observed in humans and as a result aged mice have been used more extensively than young mice.

To develop a mouse model of SARS-CoV infection with associated mortality, transgenic mice expressing human ACE2 have been generated (42, 43, 59, 60). In general, disease severity in transgenic mice correlated with the level of hACE2 expression. Transgenic mice

Author Manuscript Author Manuscript Author Manuscript Author Manuscript

expressing hACE2 under the control of a cytokeratine promoter had high levels of ACE2 mRNA in the lung, liver, colon, and kidney (42, 59). When these mice were challenged with SARS-CoV, they developed a severe infection beginning in the airway epithelium that spread to the brain. Infection resulted in weight loss beginning between days 3 to 5, and 100% mortality by day 7 (42, 59). Using an alternate approach in which hACE2 was expressed under the control of a chicken beta-actin promoter with an cytomegalovirus IE enhancer, transgenic mouse lines with differing levels of hACE2 were generated (60). Infection of mice with high levels of hACE2 expression similarly yielded a severe lung and brain infection with 100% mortality. In contrast, infection of mice expressing lower levels of hACE2 resulted in clinical illness without associated mortality (60). This finding was further supported by a third model in which hACE2 was expressed under the control of the mouse ACE2 promoter resulting in limited tissue distribution of hACE2. When these mice were challenged with SARS-CoV, they became lethargic but survived infection (43). These mice also showed severe interstitial pneumonia with extrapulmonary organ damage suggesting that they more accurately modeled human SARS-CoV infection. However, in all of these studies, an increase in viral load or viral antigen was observed in the brain tissue of transgenic mice, and mortality resulted from extensive dissemination of the virus in the brain (42). This finding is in contrast to human disease in which central nervous system infection was only rarely observed. Thus, while transgenic mice resulted in a lethal model of SARS-CoV infection, no mouse model accurately reproduced the disease spectrum observed in SARS-CoV infected patients.

Syrian Hamster Model

Golden Syrian hamsters are highly permissive to SARS-CoV infection (40, 61, 62). Infection of hamsters with SARS-CoV (10^3 or 10^5 $TCID_{50}$ of the Urbani strain) results in a productive infection with peak replication on day 2–3 in the nasal turbinates and lungs, and viral clearance by day 7. Infection also results in extrapulmonary spread consisting of transient viremia and spread to the liver and spleen in a proportion (1/3 or 2/3) of animals. Viral replication is accompanied by pulmonary histopathology consisting of focal areas of interstitial inflammation and consolidation that are visible on day 3, and become more widespread until day 7 when consolidation involves 30–40% of the lung (62). Despite the extensive pulmonary pathology, hamsters do not display overt clinical disease or mortality. Weight loss is difficult to assess in hamsters due to the storage of food in large cheek pouches; however, the use of a running wheel with a rotation counter permitted objective measurement of nocturnal activity of these animals. Compared to mock-infected hamsters and pre-infection activity levels, SARS-CoV infected hamsters exhibited a greater than 90% reduction in activity (40, 61). This was the first objective measurement of clinical illness in hamsters.

In subsequent studies, hamsters were also shown to be susceptible to several different strains of SARS-CoV (40). These strains included Urbani, HKU-39849, Frankfurt 1, and a recombinant clone GD03T0013. Infection with Frk-1 resulted in limited mortality in 3 of 20 animals, while all other strains did not produce a lethal infection. Collectively, these studies demonstrate that the hamster represents a suitable model of SARS-CoV infection; although,

Author Manuscript Author Manuscript Author Manuscript Author Manuscript

much like the young and aged mouse models, mortality was not a prominent feature of the model (63, 64).

Ferret Model

Ferrets represent an excellent model of influenza infection and as a result were evaluated for susceptibility to SARS-CoV. Infection of ferrets with virus doses from 10^3 to 10^7 $TCID_{50}$ yielded a productive infection in lungs, trachea and nasal turbinates. Viral replication peaked in the lungs on day 5 or 6, and reached levels of 10^6 $TCID_{50}$/mL of lung homogenate (65–68). The primary histopathological finding was of multifocal pulmonary lesions affecting 5–10% of the lung with mild alveolar damage, and peribronchiolar and perivascular lymphocyte infiltration (66, 67, 69). Reports on clinical disease vary. In initial studies utilizing intratracheal administration, 3 of 6 infected ferrets became lethargic and one animal succumbed to disease, and in a study utilizing the Toronto-2 (Tor2) SARS-CoV isolate, lethargy and prolonged disease was also observed (66, 70). In subsequent reports using either intratracheal or intranasal administration lethargy or mortality were not observed (65, 67, 68, 71). Furthermore, in a study specifically designed to assess the ferret as a non-rodent model to meet the criteria for the FDA “Animal Rule”, clinical disease was limited to fever and sneezing in large groups of ferrets inoculated with the Toronto-2 strain (65). In a single study, contact transmission of SARS-CoV to uninfected cage mates was reported along with conjunctivitis and mortality on days 16 and 21 (66). Histopathological analysis found evidence of hepatic lipidosis and emaciation indicating mortality was not associated with SARS-CoV pneumonia. These findings indicate that SARS-CoV could transmit at low levels by direct contact in the ferret model. In summary ferrets were shown to support SARS-CoV replication with varying degrees of clinical disease, and much like the rodent models, SARS-CoV infection did not result in significant mortality.

Non-Human Primate Models

Six NHP species have been evaluated as models of SARS-CoV infection. These include three Old World Monkeys: rhesus and cynomolgus macaques, and African Green monkeys, and three New World Monkeys: common marmoset, squirrel monkeys, and mustached tamarins (72–80). With the exception of squirrel monkeys and mustached tamarins (75), all NHPs examined support SARS-CoV replication. Initial studies were performed in cynomolgus macaques to demonstrate that SARS-CoV fulfilled Koch’s postulates. In these studies, virus was isolated from nasal secretions, and virus could be detected in lung samples by RT-PCR. Consistent with virus isolation, the animals had pulmonary pathology indicative of interstitial pneumonia and representative of mild human disease. In these and other studies using cynomolgus macaques a range of clinical illness has been reported with observations ranging from skin rash, decreased activity, cough, and respiratory distress, to an absence of clinical disease (73, 76, 77, 79).

To compare Old World monkey species, African Green monkeys, cynomolgus, and rhesus macaques were challenged in parallel with SARS-CoV Urbani strain. No animals developed clinical disease and all three species had viral replication in combined nasal-throat swabs, and in tracheal lavage samples (76). Viral replication was highest in African Green monkeys, followed by cynomolgus and then rhesus macaques. Viral titers peaked by day 2

Author Manuscript Author Manuscript Author Manuscript Author Manuscript

with clearance in the upper and lower respiratory tract by days 8 and 10, respectively. All three species produced neutralizing antibodies and antibody titers correlated with virus replication. Pulmonary pathology was examined in African Green monkeys on day 2 and 4 post-infection. Consistent with the features of interstitial pneumonia, on day 2 there were focal interstitial mononuclear inflammatory infiltrates and edema in the lung. Staining for viral antigen identified type 1 pneumocytes as the predominant cell type infected by SARS-CoV, and on day 4 there was a reduction in the amount of viral antigen and level of inflammation (76). In a subsequent study on Rhesus macaques challenged with the SARS-CoV PUMC01 strain, virus could be detected in nasal and pharyngeal swabs, and on days 5 and 7 pulmonary histopathology was similarly consistent with interstitial pneumonia (78).

Infection of common marmosets also resulted in mild clinical disease with ~50% of animals developing a febrile response and diarrhea (80). Due to technical challenges, replicating virus could not be isolated from lung homogenates; however, high levels of vRNA were detected in lung samples on both days 4 and 7 post-infection. Marmosets developed both pulmonary and hepatic pathology with evidence of interstitial pneumonitis at all time points (days 2, 4, and 7). Hepatic lesions started to develop on day 2 and were readily apparent in 4 of 5 animals on day 4. On day 7 all animals had evidence of multifocal hepatitis. Hepatic lesions were also observed in human patients and the marmoset was the only NHP to develop liver disease (80). Collectively, the NHP species that were permissive to SARS-CoV infection modeled differing aspects of human disease with African Green monkeys supporting high levels of replication in the respiratory tract and marmosets modeling hepatic pathology. All species showed evidence of interstitial pneumonia, however, no species consistently reproduced severe clinical disease and mortality was not observed in any species.

Role of ACE2 in Animal Models of SARS-CoV Infection

ACE2 was identified as the functional receptor for SARS-CoV in African Green monkey derived Vero E6 cells (37). Subsequent crystallography studies identified 14 amino acid positions in ACE2 that have direct contact with the S protein receptor-binding domain (RBD) (See Table 1) (81). As civet (c) ACE2 displayed affinity for both human (Tor2 and GD03) and civet SARS-CoV isolates (Sz02 and Gd05), while human (h) ACE2 preferentially bound the S protein RBD of human isolates, biochemical studies were performed to define mutations influencing RBD affinity (82–85). These studies identified two regions of interaction between the S protein RBD and ACE2 at which mutations evolved to accommodate a switch in preference from cACE2 to hACE2 (82, 83, 85). The two regions were designated hotspot 31 and hotspot 353. In hotspot 31, residues K31 and E35 of hACE2 interact to form a salt bridge, and E35 in turn interacts with N479 of the S protein RBD. In contrast, the RBD of civet isolates have a 479K mutation and this lysine residue competes with E35 of hACE2 destabilizing the salt bridge and diminishing binding. To compensate, civet ACE2 has a Threonine (T) at position 31. This removes the salt bridge structure and the destabilizing effect of 479K, permitting high affinity binding (82).

The interaction of amino acids at or near position 353 of ACE2 were also found to play a significant role in RBD–ACE2 affinity. Both hACE2 and cACE2 have lysine (K) at position

Author Manuscript Author Manuscript Author Manuscript Author Manuscript

353, and in hACE2 K353 interacts with aspartate (D) 38 to form a second salt bridge. Formation of this bridge requires additional support from threonine (T) 487 from the S protein RBD of human SARS-CoV strains. In civet isolates, there is a serine (S) at position 487 that does not support the formation of a salt bridge with D38, resulting in decreased affinity for hACE2. In cACE2 position 38 encodes a glutamate (E) that has a longer side chain than aspartate. This allows E38 to support the formation of a salt bridge in the absence of T487 and promotes binding of the civet isolates to cACE2 (82).

In the context of animal models of SARS-CoV infection, the interactions of the S protein RBD at these hot spots may partially explain the varying levels of replication observed in different species. In Table 1, we have compared the ACE2 amino acids that interact with the S protein RBD from several species. Examining the human, AGM, and macaque ACE2 residues, all 4 species have identical RBD-ACE2 interaction residues. The marmoset and hamster ACE2 residues are very similar to those of hACE2 and this is in agreement with the permissive nature of these species. In contrast, many of the residues of mouse ACE2 are different from those of human ACE2 (81) and this corresponds with reduced replication of SARS-CoV in mouse cells (86) and the lungs of young mice (47). While mice are semi-permissive to SARS-CoV, rats do not support replication of SARS-CoV. Two changes relative to human ACE2, at positions 353 and 82 of mouse and rat ACE2 are predicted to account for this difference in replication (81). Both mice and rats have a histidine at position 353 compared to 353K in hACE2. This partially disrupts the S protein-DPP4 interaction (81); moreover, the asparagine (N) 82 of rat ACE2 introduces a glycosylation site that blocks the interaction at position 82 with residue L472 of the S protein RBD. In contrast, mouse ACE2 has a serine (S) at position 82, that though sub-optimal, does not prevent the interaction with the S protein. Together the combined changes in mACE2 at position 353 and 82 lead to inefficient binding of the S protein and reduced permissiveness of mouse cells, while the glycosylation site at residue 82 in rat ACE2 abrogates binding (81).

Examination of the hamster ACE2 sequence at position 82 also reveals an asparagine (N) residue and examination of the surrounding amino acid residues indicates the presence of a glycosylation site. This is surprising as hamsters are highly permissive to SARS-CoV; however, the inhibitory effect of N82 may be overcome by the multiple additional interactions (i.e. K353) that are shared by human and hamster ACE2. It is tempting to speculate that hamsters may have developed lethal or more pronounced clinical disease if the amino acid residue at position 82 had been similar to that of hACE2.

Of interest, most of the ferret ACE2 interaction residues are different from those of hACE2, thus it is surprising that ferrets are permissive to SARS-CoV infection. Comparing civet and ferret ACE2, many of the residues are the same, and experimental studies have shown that civets can be infected with human isolates (87). Thus, while the ferret ACE2 may be different from hACE2, the similarity with cACE2 may result in affinity between ferret ACE2 and the S protein RBD permitting infection and replication.

In summary, the structural analysis of ACE2 – S protein interactions agree with observations of improved replication in several animal models. However, this finding does not fully explain the host restriction and limited clinical disease observed in animal models. Despite

Author Manuscript Author Manuscript Author Manuscript Author Manuscript

high degrees of similarity between NHP ACE2 sequences and hACE2, NHP's do not recapitulate human disease and within the NHP species there is variation in the level of viral replication. Furthermore, aged mice develop disease and support replication despite reduced affinity of mACE2 for the S protein RBD. Thus, while it is clear the interaction of ACE2 with the S protein-RBD is required for efficient infection and replication, additional host factors likely also contribute to the development of severe disease.

Mouse-adaptation of SARS-CoV

As an alternative to evaluating multiple animal species, another strategy to generate an animal model with clinical disease is to adapt the virus to the new host by serial passage (Figure 1). To generate a mouse model with associated mortality, the SARS-CoV Urbani strain was serially passaged in the lungs of young BALB/c mice (41). After 15 passages, a single virus clone was isolated that caused 100% mortality in young (6–8 week old), 4 week old, and aged BALB/c mice. This virus was designated MA15. Severe disease was the result of an overwhelming viral infection with significantly higher titers and prolonged replication in the lungs accompanied by extensive damage to bronchiolar and alveolar epithelial cells (41). MA15 was also capable of extrapulmonary spread as evident by viremia, and recovery of virus from spleen, liver, and brain tissues. Sequence analysis and reverse genetics studies identified 6 amino acid mutations associated with the lethal phenotype. These mutations included 3 changes in ORF1a, and single changes in ORF1b, the M protein, and the S protein. Of particular interest, the mutation in the S protein Y436H was located in the S protein RBD. In follow-up studies, the relative contribution of each mutation in MA15 was defined using a panel of recombinant viruses (88). Reversion of four mutations did not alter virulence, however, reversion of the nsp9 (located in ORF1a) or S protein mutations resulted in reduced weight loss from >20% to 10–20% and less than 5% for the nsp9 and S protein mutations, respectively. Furthermore, reversion of the S protein mutation resulted in a non-lethal infection with no clinical disease. Introduction of the S protein and nsp9 mutations either alone or combined into the Urbani infectious clone failed to induce a lethal infection in young BALB/c mice indicating that the S protein and nsp9 mutations were necessary but not sufficient to induce severe disease. Given that 6 mutations were present in MA15, the additional mutations in ORF1a, ORF1b, and the M gene may have lead to enhanced disease by promoting interactions with host cell proteins involved in viral replication (88, 89). Alternatively, these mutations may also alter the host response as $STAT^{-/-}$ mice progressed more rapidly to a terminal endpoint when inoculated with MA15 compared to wild-type virus (90).

To develop additional mouse-adapted virus strains, the Urbani strain was similarly passaged 20 or 25 times in two separate studies to yield lethal virus strains termed MA20 and Strain v2163 (88, 91). In a direct comparison with MA15, infection with Strain v2163 resulted in significantly higher pulmonary virus titers and enhanced mortality at lower doses. Ten amino acid changes in v2163 were associated with adaptation and 4 mutations arose in the S protein. More specifically, Y436H and a second mutation at Y442F were identified in the RBD. An additional mutation K411E in the RBD was found in some samples, but was not found in the lungs of infected mice. The two remaining S protein mutations were T1118I and N1169D and were located outside the RBD in the S2 heptad repeat elements (91).

Author Manuscript Author Manuscript Author Manuscript Author Manuscript

Sequencing of the MA20 strain revealed 6 amino acid mutations with two changes in the S protein binding domain: Y442L and N479K (88).

The changes that arose during mouse adaptation in the S protein RBD are predicted to enhance affinity or binding of the S protein to mACE2. In human SARS-CoV strains, residue Y436 of the S protein interacts with hACE2 at residues D38 and Q42. This interaction is within hotspot 31 and binding is further influenced by residue 353K of hACE2. In mACE2 the K353H mutation interferes with the interaction between Y436 of the S protein RBD and D38 of mACE2. Thus, in MA15, the mutation Y436H that arose with serial passage overcomes this interference (88) promoting enhanced binding. In the MA20 strain, two mutations evolved in the RBD: Y442L and N479K. These mutations are predicted to form polar interactions with N30 and N31 of mACE2, and the change of Y442L removes a bulky side chain permitting access and enhancing binding of K479 to N30 and N31 (88). The v2163 strain contains mutations, Y436H and Y442F. As described above the Y436H mutation most likely compensates for mACE2 353H. The extent of steric clash between N31 of mACE2 and Y442 has not been described; however, the Y442F change removes a hydroxyl group from the binding interface and this is predicted to enhance the interaction with mACE2 (88).

The mouse adaptation studies yielded several SARS-CoV strains capable of causing lethal disease in mice. These strains represent an advance in the development of an animal model for the “Animal Rule” though the disease mechanism in young mice is different from that in humans. The use of the MA15 virus in aged mice has proved to be a valuable model for the study of SARS-CoV vaccine candidates. Studies examining mutations that arose upon serial passage and detailed analysis of S protein ACE2 interactions emphasize the role of the S protein in host restriction and demonstrate that the S protein-host receptor interactions are critical for the development of animal models. This is further emphasized by the finding that transgenic mice expressing hACE2 and mouse-adapted SARS-CoV strains both show enhanced replication and disease. As our understanding of host-receptor interactions develops, application of this knowledge will facilitate the development animal models for emerging coronaviruses.

Animal Models of MERS Coronavirus

Mouse Models

Both wild-type mice and knockout strains have been evaluated as models of MERS-CoV infection (92). In these studies, eight week-old BALB/c, 129SvEv, and 129SvEv STAT1$^{-/-}$ mice were intranasally inoculated with 120 or 1200 $TCID_{50}$ of EMC-2012. None of the mice lost weight or developed clinical signs, and all of the mice survived challenge. On days 2 and 4 post-infection, lungs were harvested and viral load was assayed by titration on Vero cells or by qRT-PCR. RT-PCR analysis for genomic RNA indicated that the virus was present on day 2; however, no subgenomic mRNA transcripts, indicative of active replication, were detected and replicating virus could not be cultured from lung homogenates. Furthermore, mice did not develop pulmonary pathology (92). Analysis of the MERS-CoV host receptor (DPP4) expression by immunohistochemistry and RT-PCR indicated that low levels of DPP4 were expressed in the lungs (92), and early studies on the

Author Manuscript Author Manuscript Author Manuscript Author Manuscript

binding efficiency of MERS-CoV S protein RBD to mouse cells (LR7 cell line) showed low binding efficiency (See Table S1 of (39)). Collectively, these studies demonstrated that mice are naturally non-permissive to MERS-CoV and inbred strains do not represent a suitable small animal model.

Syrian Hamster Model

Based on the success of hamsters as a model for SARS-CoV, they were similarly evaluated as a model of MERS-CoV infection (93). Syrian hamsters were given either 10^3 or 10^6 $TCID_{50}$ of EMC-2012 by intratracheal inoculation or 4×10^2 $TCID_{50}$ via aerosol. Animals were monitored for clinical disease, and nasal, oropharyngeal, urogenital, and rectal swabs were collected daily from days 1–11 post-infection. Inoculated animals did not display clinical signs or weight loss, and all swabs were negative for viral RNA by qRT-PCR (93). Tissues were collected on days 2, 4, 8, 14, and 21 post-infection. On days 2, 4, and 8, vRNA could not be detected in the lungs, spleen, or mandibular lymph nodes by qRT-PCR, and no significant histopathology was observed in the lungs, trachea, kidney, and brain. To further determine if the hamsters had been infected, Mx gene expression was assayed as an indicator of an innate immune response. In MERS-CoV inoculated animals, Mx expression was similar to that of mock-infected infected animals. To verify that the host receptor of MERS-CoV was expressed in hamsters, immunohistochemistry for DPP4 was performed. DPP4 was expressed at high levels in bronchiolar epithelium and smooth muscle in the lung, and also in the glomerular parietal epithelium and nerve tissue in the kidney (93). Collectively, these results indicate that similar to mice, hamsters are not permissive to MERS-CoV; however, in contrast to mice, hamsters do show high levels of DPP4 expression.

Ferret Model

To potentially overcome host factors that may limit infection in rodents, ferrets were evaluated as a model for MERS-CoV (94). Four animals were inoculated intranasally and intratracheally with 1×10^6 $TCID_{50}$ of EMC-2012. Nasal and throat swabs were collected at intervals from 1 to 14 days post-infection and assayed for viral replication. Virus was not recovered from the swabs and qRT-PCR analysis demonstrated that low levels of viral RNA were present only on days 1 and 2 post-infection (94). Ferrets also failed to seroconvert, further evidence that the animals had not been infected. In subsequent experiments, primary ferret kidney cells were shown to be resistant to MERS-CoV infection despite high levels of DPP4 expression. Transfection of an expression plasmid for human DPP4 into primary ferret kidney cells rendered the cells susceptible to MERS-CoV infection, demonstrating that ferret DPP4 was the major host restriction factor. Further *in vitro* experiments with chimeric human-ferret DPP4 constructs demonstrated that the DPP4 receptor-binding domain (RBD) was responsible for the relative resistance or susceptibility of ferret cells to infection with MERS-CoV (94). These findings demonstrate that ferrets, like hamsters and mice, are not a suitable as a model of MERS-CoV infection.

Author Manuscript Author Manuscript Author Manuscript Author Manuscript

Non-human primate models

Two species of NHP have been evaluated as models of MERS-CoV infection. These include the rhesus macaque and common marmoset (95–98). Both species are susceptible to MERS-CoV infection; however, the extent of replication and disease severity vary. Upon a combined intranasal, intratracheal, oral and ocular inoculation with 1×10^7 $TCID_{50}$ EMC-2012 strain, Rhesus macaques develop mild clinical signs consisting of decreased food intake, nasal swelling, increased respiratory rate, and elevated white blood cells counts early after infection (days 1–2 p.i.) (95, 97). All animals survived until the designated endpoint of day 6 post-infection. vRNA was detected in nasal swabs on days 1 and 3, and in most animals was cleared by day 6. Replicating virus could be recovered from lung tissue (97) and titers decreased from day 3 to 6 post-infection. Examination of viral dissemination throughout the respiratory tract by qRT-PCR demonstrated that vRNA could be detected in the nasal mucosa, trachea, mediastinal lymph nodes, conjunctiva, oronasopharynx, and bronchi on day 3. Viral loads decreased by day 6 and vRNA could not be detected in the nasal mucosa and conjunctiva at this later time point (95). Gross examination of multiple organs on day 3 and 6 revealed that pathology was restricted to the lungs with 0–75% of each lung lobe containing lesions. Consistent with this observation, vRNA could not be detected in the kidney or bladder. Further histopathological analysis found that animals displayed mild to marked interstitial pneumonia on day 3 that progressed to abundant alveolar edema and formation of hyaline membranes on day 6 (95, 97).

In an analogous study, four rhesus macaques were intratracheally inoculated with 6.5×10^7 $TCID_{50}$ of EMC-2012. Two animals were maintained for 28 days and two animals were necropsied on day 3 p.i. All of the animals showed an increase in temperature on days 1–2, had reduced water intake, and survived the infection. RNA was not detected in nasal, oropharyngeal, and cloacal swabs collected at regular intervals. Radiographic imaging on days 3 and 5 showed interstitial infiltrates indicative of pneumonia, and replicating virus was isolated from lung samples on day 3. Virus could not be isolated from any other tissue including trachea, brain, and kidney (98). Similar to the previous study, gross examination revealed lesions restricted to the lung, and microscopic analysis showed multifocal mild to moderate interstitial pneumonia. Animals also developed serum neutralizing antibody responses that were detected on day 7, peaked on day 14 (1:320) and remained elevated at day 28 (1:160)(98).

Taken together, these studies show that infection of rhesus macaques with MERS-CoV results in a transient lung infection with associated pneumonia. The discrepancies in the extent of virus replication in the respiratory tract, observations of nasal swelling, and isolation of virus from nasal swabs most likely reflect the use of multiple inoculation routes in the earlier studies. Animals showed mild clinical disease early during infection and mortality was not observed. Thus, rhesus macaques do not recapitulate the severe infection observed in human cases; however, IFN-α and ribavirin were evaluated in this model and were shown to limit infection (99).

Based on modeling of MERS-CoV S protein-DPP4 interactions, the common marmoset was evaluated as model of MERS-CoV (96). To recapitulate severe disease marmosets were given a total of 5.2×10^6 $TCID_{50}$ of EMC-2012 via a combination of intranasal, oral, ocular,

Author Manuscript Author Manuscript Author Manuscript Author Manuscript

and intratracheal routes. Clinical disease ranged from moderate to severe, with animals showing increased respiratory rate, decreased body temperature, loss of appetite, and decreased activity. Peak clinical illness was observed between day 4 and 6, and 2 of nine animals were euthanized due to severe disease. Radiological evaluation revealed evidence of moderate to severe interstitial infiltration in both lower lung lobes on day 3 and 6; by day 9 the remaining animals had reduced infiltration indicative of recovery. On day 1 all throat swabs and 8/9 nasal swabs were positive for vRNA. Viral load in the nose and throat swabs decreased by day 3, but vRNA was consistently isolated from throat swabs in a proportion of animals as late as 13 days post-infection. In the respiratory tract, vRNA could be detected from days 2–6 in the conjunctiva, nasal mucosa, trachea, mediastinal lymph node, and all lung lobes. In addition, two animals showed evidence of viremia with vRNA detected in the blood and vRNA was detected in multiple organs including the kidney, liver, and heart, indicating systemic dissemination of the virus. However, given that the animals were inoculated via multiple routes this may have facilitated systemic infection and spread throughout the respiratory tract.

Histopathological analysis on day 3 revealed acute bronchointerstitial pnemonia with viral antigen present in regions of pathological change. By day 6, acute pneumonia was still prominent, with type II pneumocyte hyperplasia and consolidation of pulmonary fibrin resulting in hyaline membrane formation. Consistent with the severe lung infection, type I pneumocytes, bronchiolar epithelial cells, and smooth muscle cells were all found to express DPP4 (96). Thus, the common marmoset reproduces several features of MERS-CoV infection, and can potentially be used to evaluate novel therapies for human use.

Role of Host Receptor DPP4 in Animal Models of MERS-CoV

To understand the restriction of MERS-CoV replication in small animals, evidence of host restriction at the level of DPP4 sequence was sought. The crystal structure of the S protein bound to DPP4 has been solved (100, 101). At the interface between the S protein RBD and DPP4, 14 residues of the S protein RBD have direct contact with 15 residues of hDPP4 (See Table 2) (100). The interaction between DPP4 and the S protein RBD has two major binding patches. Patch 1 consists of hDPP4 residues K267 and R336 interacting with a negatively charged surface consisting of E536, D537, and D539 of the S protein RBD. In addition, Y499 of the S protein RBD forms a hydrogen bond with R336 of DPP4 (100, 101). The second major binding patch consists of DPP4 residues L294, I295, H298, R317, and Q344. Residues L294 and I295 interact with S protein RBD residues L506, W553, and V555, and DPP4 residues R317 and Q344 form a salt-bridge and hydrogen bond with S protein RBD residues D510 and E513, respectively.

As mentioned above, initial studies with chimeric DPP4 proteins demonstrated that incorporation of the human DPP4 S protein RBD (residues 246–505) into ferret DPP4 rendered ferret cells susceptible to MERS-CoV infection (94). To further understand the role of the S protein RBD in host restriction, subsequent studies compared the MERS-CoV S protein binding affinity of human and mouse DPP4, and that of several potential zoonotic reservoir species including camels, horses, goats, and bats (102). Introduction of the human DPP4 S protein binding domain into mouse DPP4 rendered mouse cells susceptible to

Author Manuscript Author Manuscript Author Manuscript Author Manuscript

MERS-CoV infection, thus emphasizing the role of the DPP4 sequence in host restriction. Comparison of human DPP4 binding affinity to that other species demonstrated that human DPP4 had the highest affinity for the S protein RBD, and affinity decreased as follows: human>horses>camels>goats>bats. Expression of DPP4 from all these species rendered cells susceptible to infection, while mouse DPP4 did not permit infection (102). Further characterization of amino acid residues at the interface of DPP4 with the S protein RBD identified 6 differences between mouse and human DPP4 (See Table 2) (102–104). Structural modeling predicted that five amino acid differences at residues 288[282], 294[288], 295[289], 336[330], and 346[340] (human [mouse] DPP4 numbering) account for the lack of binding affinity in mouse DPP4 (104). Introduction of the human DPP4 residues at all 5 sites in mouse DPP4 resulted in highly efficient infection. Selective mutation of only residues 336 and 346 associated with the patch 1 binding region, or residues 288, 294, 295 in the patch 2 domain did not restore highly efficient infection, indicating that interactions with both patch regions were required for high affinity DPP4-S protein binding. In support of this finding, the introduction of human residues A294L and T330R associated with patch 1 and 2, respectively, resulted in efficient infection (104).

In the context of the hamster model, expression of human DPP4 in non-permissive (BHK) hamster cells, rendered cells susceptible to MERS-CoV infection, indicating that host restriction occurred at the level of the receptor (103). Comparison of the hamster and human DPP4 sequences identified five amino acid differences in the DPP4 S protein RBD interface (Table 2) (103). Introduction of the human residues into hamster DPP4 permitted infection of hamster cells, and modeling studies suggested that two residues at positions 291 and 336 were largely responsible for the host restriction (103). This is in agreement with studies on mouse DPP4 that show mutation R336T, also present in the hamster DPP4, decreases infection by MERS-CoV (104).

Collectively, these studies demonstrate that host restriction of MERS-CoV is predominantly dictated by DPP4 sequence. To explore additional animal models we sequenced cotton rat DPP4 (See Table 2) and found the S protein binding residues to be similar to those of the hamster and ferret, suggesting that cotton rats would be refractory to infection. Indeed comparison of human, rhesus macaque and common marmoset DPP4 sequences show 100% identity at the residues that interact with MERS-CoV S protein. However, the differences in disease severity between rhesus macaques and common marmosets indicate that other host factors such as the presence or expression levels of S-cleaving proteases (i.e. TMPRSS2) (104) may influence infection and disease severity. Regardless of additional host factors, the interaction of DPP4 with MERS-CoV S protein should be the initial and predominant focus of small animal model development.

Approaches to Developing Small Animal Models of MERS-CoV Infection

Development of animal models for SARS-CoV demonstrated that both mouse adaptation and the generation of transgenic mice expressing hACE2 resulted in enhanced permissiveness and disease. Moving forward with animal models of MERS-CoV, similar strategies should be utilized. Mouse adaptation, or adaptation to ferrets or hamsters, are unlikely to be fruitful approaches because infectious virus could not be isolated from these

Author Manuscript Author Manuscript Author Manuscript Author Manuscript

animals and the MERS-CoV S protein failed to bind DPP4 from these species. To overcome this barrier, reverse genetics approaches could be used to introduce mutations into the MERS-CoV S protein RBD to enhance or promote interaction with DPP4 of different species. This has particular utility in outbred animals in which genetic manipulation of the host receptor would be challenging.

As demonstrated with SARS-CoV, the generation of mice expressing human DPP4 may be the most rapid strategy to yield a small animal model. Indeed, when mice were transduced with an adenovirus vector that expressed human DPP4, they were susceptible to MERS-CoV infection and developed pneumonia, albeit without associated mortality (105). Transgenic mice could be generated via traditional methods or using the CRISPR-Cas9 (106) system to replace mouse DPP4 with human DPP4 or to introduce a mouse DPP4 carrying the mutations that promote S protein binding. With either transgenic strategy or with the development of a reverse genetics adapted strain, replication and pathogenesis will have to be characterized to meet the criteria for the FDA Animal Rule.

Despite the lack of suitable models, several groups are developing vaccines and therapeutics against MERS-CoV (107–114). Vaccine candidates are being evaluated for immunogenicity and antivirals are being evaluated *in vitro*. Medical countermeasures have the potential to advance along the path towards regulatory approval if a susceptible small animal model can be developed and used in conjunction with the marmoset model. In concert with public health efforts, novel therapies could curb the on-going MERS-CoV epidemic and reduce the morbidity and mortality associated with MERS-CoV.

Acknowledgments

Research in the authors lab was supported by the Intramural Research Program of the NIH, NIAID.

References

1. Severe acute respiratory syndrome (SARS). Releve epidemiologique hebdomadaire / Section d'hygiene du Secretariat de la Societe des Nations = Weekly epidemiological record / Health Section of the Secretariat of the League of Nations. 2003; 78(12):81–83.
2. Chinese SMEC. Molecular evolution of the SARS coronavirus during the course of the SARS epidemic in China. Science. 2004; 303(5664):1666–1669. [PubMed: 14752165]
3. Zhong NS, Zheng BJ, Li YM, Poon, Xie ZH, Chan KH, et al. Epidemiology and cause of severe acute respiratory syndrome (SARS) in Guangdong, People's Republic of China, in February, 2003. Lancet. 2003; 362(9393):1353–1358. [PubMed: 14585636]
4. Peiris JS, Lai ST, Poon LL, Guan Y, Yam LY, Lim W, et al. Coronavirus as a possible cause of severe acute respiratory syndrome. Lancet. 2003; 361(9366):1319–1325. [PubMed: 12711465]
5. Tsang KW, Ho PL, Ooi GC, Yee WK, Wang T, Chan-Yeung M, et al. A cluster of cases of severe acute respiratory syndrome in Hong Kong. The New England journal of medicine. 2003; 348(20): 1977–1985. [PubMed: 12671062]
6. Poutanen SM, Low DE, Henry B, Finkelstein S, Rose D, Green K, et al. Identification of severe acute respiratory syndrome in Canada. The New England journal of medicine. 2003; 348(20):1995–2005. [PubMed: 12671061]
7. Ruan YJ, Wei CL, Ee AL, Vega VB, Thoreau H, Su ST, et al. Comparative full-length genome sequence analysis of 14 SARS coronavirus isolates and common mutations associated with putative origins of infection. Lancet. 2003; 361(9371):1779–1785. [PubMed: 12781537]

Author Manuscript Author Manuscript Author Manuscript Author Manuscript

8. Ksiazek TG, Erdman D, Goldsmith CS, Zaki SR, Peret T, Emery S, et al. A novel coronavirus associated with severe acute respiratory syndrome. The New England journal of medicine. 2003; 348(20):1953–1966. [PubMed: 12690092]

9. WHO. Cumulative Number of Reported Probable Cases of SARS. 2003. [updated July 11, 2003]. Available from: http://www.who.int/entity/csr/sars/country/2003_07_11/en/index.html

10. WHO. World Health Organization issues emergency travel advisory. 2003. Available from: http://www.who.int/csr/sars/archive/2003_03_15/en/

11. Booth CM, Matukas LM, Tomlinson GA, Rachlis AR, Rose DB, Dwosh HA, et al. Clinical features and short-term outcomes of 144 patients with SARS in the greater Toronto area. Jama. 2003; 289(21):2801–2809. [PubMed: 12734147]

12. Chan JW, Ng CK, Chan YH, Mok TY, Lee S, Chu SY, et al. Short term outcome and risk factors for adverse clinical outcomes in adults with severe acute respiratory syndrome (SARS). Thorax. 2003; 58(8):686–689. [PubMed: 12885985]

13. Donnelly CA, Ghani AC, Leung GM, Hedley AJ, Fraser C, Riley S, et al. Epidemiological determinants of spread of causal agent of severe acute respiratory syndrome in Hong Kong. Lancet. 2003; 361(9371):1761–1766. [PubMed: 12781533]

14. Karlberg J, Chong DS, Lai WY. Do men have a higher case fatality rate of severe acute respiratory syndrome than women do? American journal of epidemiology. 2004; 159(3):229–231. [PubMed: 14742282]

15. Normile D, Vogel G. Infectious diseases Early indications point to lab infection in new SARS case. Science. 2003; 301(5640):1642–1643. [PubMed: 14500944]

16. Normile D. Infectious diseases Second lab accident fuels fears about SARS. Science. 2004; 303(5654):26. [PubMed: 14704402]

17. Liang G, Chen Q, Xu J, Liu Y, Lim W, Peiris JS, et al. Laboratory diagnosis of four recent sporadic cases of community-acquired SARS, Guangdong Province, China. Emerging infectious diseases. 2004; 10(10):1774–1781. [PubMed: 15504263]

18. Ge XY, Li JL, Yang XL, Chmura AA, Zhu G, Epstein JH, et al. Isolation and characterization of a bat SARS-like coronavirus that uses the ACE2 receptor. Nature. 2013; 503(7477):535–538. [PubMed: 24172901]

19. Lau SK, Woo PC, Li KS, Huang Y, Tsoi HW, Wong BH, et al. Severe acute respiratory syndrome coronavirus-like virus in Chinese horseshoe bats. Proceedings of the National Academy of Sciences of the United States of America. 2005; 102(39):14040–14045. [PubMed: 16169905]

20. Zaki AM, van Boheemen S, Bestebroer TM, Osterhaus AD, Fouchier RA. Isolation of a novel coronavirus from a man with pneumonia in Saudi Arabia. The New England journal of medicine. 2012; 367(19):1814–1820. [PubMed: 23075143]

21. Bermingham A, Chand MA, Brown CS, Aarons E, Tong C, Langrish C, et al. Severe respiratory illness caused by a novel coronavirus, in a patient transferred to the United Kingdom from the Middle East, September 2012. Euro surveillance : bulletin Europeen sur les maladies transmissibles = European communicable disease bulletin. 2012; 17(40):20290. [PubMed: 23078800]

22. WHO. [cited 2014 December 11, 2014] Middle East respiratory syndrome coronavirus (MERS-CoV) – update May 9, 2014. 2014. updated May 9, 2014. Available from: http://www.who.int/csr/disease/coronavirus_infections/MERS_CoV_Update_09_May_2014.pdf?ua=1

23. Al-Tawfiq JA, Memish ZA. Middle East respiratory syndrome coronavirus: epidemiology and disease control measures. Infection and drug resistance. 2014; 7:281–287. [PubMed: 25395865]

24. ECDC. Communicable DIsease Threats Report Week 50, 7–13 December [Report]. Sweden: European Centre for Disease Prevention and Control; 2014. Available from: http://ecdc.europa.eu/en/publications/Publications/communicable-disease-threats-report-13-dec-2014.pdf [cited 2014 December 14, 2014]

25. Reusken CB, Haagmans BL, Muller MA, Gutierrez C, Godeke GJ, Meyer B, et al. Middle East respiratory syndrome coronavirus neutralising serum antibodies in dromedary camels: a comparative serological study. The Lancet Infectious diseases. 2013; 13(10):859–866. [PubMed: 23933067]

Author Manuscript Author Manuscript Author Manuscript Author Manuscript

26. Reusken CB, Ababneh M, Raj VS, Meyer B, Eljarah A, Abutarbush S, et al. Middle East Respiratory Syndrome coronavirus (MERS-CoV) serology in major livestock species in an affected region in Jordan, June to September 2013. Euro surveillance : bulletin Europeen sur les maladies transmissibles = European communicable disease bulletin. 2013; 18(50):20662. [PubMed: 24342516]
27. Meyer B, Muller MA, Corman VM, Reusken CB, Ritz D, Godeke GJ, et al. Antibodies against MERS coronavirus in dromedary camels, United Arab Emirates, 2003 and 2013. Emerging infectious diseases. 2014; 20(4):552–559. [PubMed: 24655412]
28. Nowotny N, Kolodziejek J. Middle East respiratory syndrome coronavirus (MERS-CoV) in dromedary camels, Oman, 2013. Euro surveillance : bulletin Europeen sur les maladies transmissibles = European communicable disease bulletin. 2014; 19(16):20781. [PubMed: 24786259]
29. Alagaili AN, Briese T, Mishra N, Kapoor V, Sameroff SC, Burbelo PD, et al. Middle East respiratory syndrome coronavirus infection in dromedary camels in Saudi Arabia. mBio. 2014; 5(2):e00884–e00814. [PubMed: 24570370]
30. Hemida MG, Perera RA, Wang P, Alhammadi MA, Siu LY, Li M, et al. Middle East Respiratory Syndrome (MERS) coronavirus seroprevalence in domestic livestock in Saudi Arabia, 2010 to 2013. Euro surveillance : bulletin Europeen sur les maladies transmissibles = European communicable disease bulletin. 2013; 18(50):20659. [PubMed: 24342517]
31. Haagmans BL, Al Dhahiry SH, Reusken CB, Raj VS, Galiano M, Myers R, et al. Middle East respiratory syndrome coronavirus in dromedary camels: an outbreak investigation. The Lancet Infectious diseases. 2014; 14(2):140–145. [PubMed: 24355866]
32. Memish ZA, Cotten M, Meyer B, Watson SJ, Alsahafi AJ, Al Rabeeah AA, et al. Human infection with MERS coronavirus after exposure to infected camels, Saudi Arabia, 2013. Emerging infectious diseases. 2014; 20(6):1012–1015. [PubMed: 24857749]
33. Azhar EI, El-Kafrawy SA, Farraj SA, Hassan AM, Al-Saeed MS, Hashem AM, et al. Evidence for camel-to-human transmission of MERS coronavirus. The New England journal of medicine. 2014; 370(26):2499–2505. [PubMed: 24896817]
34. Adney RR, van Doremalen N, VBrown VR, Bushmater T, Scott D, de Wit E, et al. Replication and Shedding of MERS-CoV in Upper Respiratory Tract of Inoculated Dromedary Camels. Emerging infectious diseases. 2014; 20(12):1999–2005. [PubMed: 25418529]
35. Masters, PS.; Perlman, S. Coronaviruses. In: Knipe, DM.; Howley, PM., editors. Fields Virology. Vol. 6. Lippincott Williams; 2013. p. 825-858.
36. van Boheemen S, de Graaf M, Lauber C, Bestebroer TM, Raj VS, Zaki AM, et al. Genomic characterization of a newly discovered coronavirus associated with acute respiratory distress syndrome in humans. mBio. 2012; 3(6)
37. Li W, Moore MJ, Vasilieva N, Sui J, Wong SK, Berne MA, et al. Angiotensin-converting enzyme 2 is a functional receptor for the SARS coronavirus. Nature. 2003; 426(6965):450–454. [PubMed: 14647384]
38. Jeffers SA, Tusell SM, Gillim-Ross L, Hemmila EM, Achenbach JE, Babcock GJ, et al. CD209L (L-SIGN) is a receptor for severe acute respiratory syndrome coronavirus. Proceedings of the National Academy of Sciences of the United States of America. 2004; 101(44):15748–15753. [PubMed: 15496474]
39. Raj VS, Mou H, Smits SL, Dekkers DH, Muller MA, Dijkman R, et al. Dipeptidyl peptidase 4 is a functional receptor for the emerging human coronavirus-EMC. Nature. 2013; 495(7440):251–254. [PubMed: 23486063]
40. Roberts A, Lamirande EW, Vogel L, Jackson JP, Paddock CD, Guarner J, et al. Animal models and vaccines for SARS-CoV infection. Virus research. 2008; 133(1):20–32. [PubMed: 17499378]
41. Roberts A, Deming D, Paddock CD, Cheng A, Yount B, Vogel L, et al. A mouse-adapted SARS-coronavirus causes disease and mortality in BALB/c mice. PLoS pathogens. 2007; 3(1):e5. [PubMed: 17222058]
42. McCray PB Jr, Pewe L, Wohlford-Lenane C, Hickey M, Manzel L, Shi L, et al. Lethal infection of K18-hACE2 mice infected with severe acute respiratory syndrome coronavirus. Journal of virology. 2007; 81(2):813–821. [PubMed: 17079315]

Author Manuscript Author Manuscript Author Manuscript Author Manuscript

43. Yang XH, Deng W, Tong Z, Liu YX, Zhang LF, Zhu H, et al. Mice transgenic for human angiotensin-converting enzyme 2 provide a model for SARS coronavirus infection. Comparative medicine. 2007; 57(5):450–459. [PubMed: 17974127]
44. Hilgenfeld R, Peiris M. From SARS to MERS: 10 years of research on highly pathogenic human coronaviruses. Antiviral research. 2013; 100(1):286–295. [PubMed: 24012996]
45. Graham RL, Donaldson EF, Baric RS. A decade after SARS: strategies for controlling emerging coronaviruses. Nature reviews Microbiology. 2013; 11(12):836–848. [PubMed: 24217413]
46. (FDA) FaDA. Services UDoHaH, editor. Silver Spring MD; 2014 May. Guidance for Industry Product Development Under the Animal Rule. ed. 2014
47. Subbarao K, McAuliffe J, Vogel L, Fahle G, Fischer S, Tatti K, et al. Prior infection and passive transfer of neutralizing antibody prevent replication of severe acute respiratory syndrome coronavirus in the respiratory tract of mice. Journal of virology. 2004; 78(7):3572–3577. [PubMed: 15016880]
48. Yang ZY, Kong WP, Huang Y, Roberts A, Murphy BR, Subbarao K, et al. A DNA vaccine induces SARS coronavirus neutralization and protective immunity in mice. Nature. 2004; 428(6982):561–564. [PubMed: 15024391]
49. Bisht H, Roberts A, Vogel L, Bukreyev A, Collins PL, Murphy BR, et al. Severe acute respiratory syndrome coronavirus spike protein expressed by attenuated vaccinia virus protectively immunizes mice. Proceedings of the National Academy of Sciences of the United States of America. 2004; 101(17):6641–6646. [PubMed: 15096611]
50. Buchholz UJ, Bukreyev A, Yang L, Lamirande EW, Murphy BR, Subbarao K, et al. Contributions of the structural proteins of severe acute respiratory syndrome coronavirus to protective immunity. Proceedings of the National Academy of Sciences of the United States of America. 2004; 101(26): 9804–9809. [PubMed: 15210961]
51. Roberts A, Thomas WD, Guarner J, Lamirande EW, Babcock GJ, Greenough TC, et al. Therapy with a severe acute respiratory syndrome-associated coronavirus-neutralizing human monoclonal antibody reduces disease severity and viral burden in golden Syrian hamsters. The Journal of infectious diseases. 2006; 193(5):685–692. [PubMed: 16453264]
52. Glass WG, Subbarao K, Murphy B, Murphy PM. Mechanisms of host defense following severe acute respiratory syndrome-coronavirus (SARS-CoV) pulmonary infection of mice. Journal of immunology. 2004; 173(6):4030–4039.
53. Hogan RJ, Gao G, Rowe T, Bell P, Flieder D, Paragas J, et al. Resolution of primary severe acute respiratory syndrome-associated coronavirus infection requires Stat1. Journal of virology. 2004; 78(20):11416–11421. [PubMed: 15452265]
54. Wentworth DE, Gillim-Ross L, Espina N, Bernard KA. Mice susceptible to SARS coronavirus. Emerging infectious diseases. 2004; 10(7):1293–1296. [PubMed: 15324552]
55. Ding Y, Wang H, Shen H, Li Z, Geng J, Han H, et al. The clinical pathology of severe acute respiratory syndrome (SARS): a report from China. The Journal of pathology. 2003; 200(3):282–289. [PubMed: 12845623]
56. Franks TJ, Chong PY, Chui P, Galvin JR, Lourens RM, Reid AH, et al. Lung pathology of severe acute respiratory syndrome (SARS): a study of 8 autopsy cases from Singapore. Human pathology. 2003; 34(8):743–748. [PubMed: 14506633]
57. Nicholls JM, Poon LL, Lee KC, Ng WF, Lai ST, Leung CY, et al. Lung pathology of fatal severe acute respiratory syndrome. Lancet. 2003; 361(9371):1773–1778. [PubMed: 12781536]
58. Roberts A, Paddock C, Vogel L, Butler E, Zaki S, Subbarao K. Aged BALB/c mice as a model for increased severity of severe acute respiratory syndrome in elderly humans. Journal of virology. 2005; 79(9):5833–5838. [PubMed: 15827197]
59. Netland J, Meyerholz DK, Moore S, Cassell M, Perlman S. Severe acute respiratory syndrome coronavirus infection causes neuronal death in the absence of encephalitis in mice transgenic for human ACE2. Journal of virology. 2008; 82(15):7264–7275. [PubMed: 18495771]
60. Tseng CT, Huang C, Newman P, Wang N, Narayanan K, Watts DM, et al. Severe acute respiratory syndrome coronavirus infection of mice transgenic for the human Angiotensin-converting enzyme 2 virus receptor. Journal of virology. 2007; 81(3):1162–1173. [PubMed: 17108019]

Author Manuscript Author Manuscript Author Manuscript Author Manuscript

61. Lamirande EW, DeDiego ML, Roberts A, Jackson JP, Alvarez E, Sheahan T, et al. A live attenuated severe acute respiratory syndrome coronavirus is immunogenic and efficacious in golden Syrian hamsters. Journal of virology. 2008; 82(15):7721–7724. [PubMed: 18463152]
62. Roberts A, Vogel L, Guarner J, Hayes N, Murphy B, Zaki S, et al. Severe acute respiratory syndrome coronavirus infection of golden Syrian hamsters. Journal of virology. 2005; 79(1):503–511. [PubMed: 15596843]
63. Liang L, He C, Lei M, Li S, Hao Y, Zhu H, et al. Pathology of guinea pigs experimentally infected with a novel reovirus and coronavirus isolated from SARS patients. DNA and cell biology. 2005; 24(8):485–490. [PubMed: 16101345]
64. Watts DM, Peters CJ, Newman P, Wang N, Yoshikawa N, Tseng CK, et al. Evaluation of cotton rats as a model for severe acute respiratory syndrome. Vector borne and zoonotic diseases. 2008; 8(3):339–344. [PubMed: 18447621]
65. Chu YK, Ali GD, Jia F, Li Q, Kelvin D, Couch RC, et al. The SARS-CoV ferret model in an infection-challenge study. Virology. 2008; 374(1):151–163. [PubMed: 18234270]
66. Martina BE, Haagmans BL, Kuiken T, Fouchier RA, Rimmelzwaan GF, Van Amerongen G, et al. Virology: SARS virus infection of cats and ferrets. Nature. 2003; 425(6961):915. [PubMed: 14586458]
67. ter Meulen J, Bakker AB, van den Brink EN, Weverling GJ, Martina BE, Haagmans BL, et al. Human monoclonal antibody as prophylaxis for SARS coronavirus infection in ferrets. Lancet. 2004; 363(9427):2139–2141. [PubMed: 15220038]
68. Weingartl H, Czub M, Czub S, Neufeld J, Marszal P, Gren J, et al. Immunization with modified vaccinia virus Ankara-based recombinant vaccine against severe acute respiratory syndrome is associated with enhanced hepatitis in ferrets. Journal of virology. 2004; 78(22):12672–12676. [PubMed: 15507655]
69. van den Brand JM, Haagmans BL, Leijten L, van Riel D, Martina BE, Osterhaus AD, et al. Pathology of experimental SARS coronavirus infection in cats and ferrets. Veterinary pathology. 2008; 45(4):551–562. [PubMed: 18587105]
70. Kobinger GP, Figueredo JM, Rowe T, Zhi Y, Gao G, Sanmiguel JC, et al. Adenovirus-based vaccine prevents pneumonia in ferrets challenged with the SARS coronavirus and stimulates robust immune responses in macaques. Vaccine. 2007; 25(28):5220–5231. [PubMed: 17559989]
71. Darnell ME, Plant EP, Watanabe H, Byrum R, St Claire M, Ward JM, et al. Severe acute respiratory syndrome coronavirus infection in vaccinated ferrets. The Journal of infectious diseases. 2007; 196(9):1329–1338. [PubMed: 17922397]
72. Kuiken T, Fouchier RA, Schutten M, Rimmelzwaan GF, van Amerongen G, van Riel D, et al. Newly discovered coronavirus as the primary cause of severe acute respiratory syndrome. Lancet. 2003; 362(9380):263–270. [PubMed: 12892955]
73. Lawler JV, Endy TP, Hensley LE, Garrison A, Fritz EA, Lesar M, et al. Cynomolgus macaque as an animal model for severe acute respiratory syndrome. PLoS medicine. 2006; 3(5):e149. [PubMed: 16605302]
74. Fouchier RA, Kuiken T, Schutten M, van Amerongen G, van Doornum GJ, van den Hoogen BG, et al. Aetiology: Koch's postulates fulfilled for SARS virus. Nature. 2003; 423(6937):240. [PubMed: 12748632]
75. Roberts A, Subbarao K. Animal models for SARS. Advances in experimental medicine and biology. 2006; 581:463–471. [PubMed: 17037579]
76. McAuliffe J, Vogel L, Roberts A, Fahle G, Fischer S, Shieh WJ, et al. Replication of SARS coronavirus administered into the respiratory tract of African Green, rhesus and cynomolgus monkeys. Virology. 2004; 330(1):8–15. [PubMed: 15527829]
77. Rowe T, Gao G, Hogan RJ, Crystal RG, Voss TG, Grant RL, et al. Macaque model for severe acute respiratory syndrome. Journal of virology. 2004; 78(20):11401–11404. [PubMed: 15452262]
78. Qin C, Wang J, Wei Q, She M, Marasco WA, Jiang H, et al. An animal model of SARS produced by infection of Macaca mulatta with SARS coronavirus. The Journal of pathology. 2005; 206(3): 251–259. [PubMed: 15892035]

Author Manuscript Author Manuscript Author Manuscript Author Manuscript

79. Rockx B, Feldmann F, Brining D, Gardner D, LaCasse R, Kercher L, et al. Comparative pathogenesis of three human and zoonotic SARS-CoV strains in cynomolgus macaques. PloS one. 2011; 6(4):e18558. [PubMed: 21533129]

80. Greenough TC, Carville A, Coderre J, Somasundaran M, Sullivan JL, Luzuriaga K, et al. Pneumonitis and multi-organ system disease in common marmosets (Callithrix jacchus) infected with the severe acute respiratory syndrome-associated coronavirus. The American journal of pathology. 2005; 167(2):455–463. [PubMed: 16049331]

81. Li F, Li W, Farzan M, Harrison SC. Structure of SARS coronavirus spike receptor-binding domain complexed with receptor. Science. 2005; 309(5742):1864–1868. [PubMed: 16166518]

82. Li F. Structural analysis of major species barriers between humans and palm civets for severe acute respiratory syndrome coronavirus infections. Journal of virology. 2008; 82(14):6984–6991. [PubMed: 18448527]

83. Wu K, Peng G, Wilken M, Geraghty RJ, Li F. Mechanisms of host receptor adaptation by severe acute respiratory syndrome coronavirus. The Journal of biological chemistry. 2012; 287(12):8904–8911. [PubMed: 22291007]

84. Li W, Zhang C, Sui J, Kuhn JH, Moore MJ, Luo S, et al. Receptor and viral determinants of SARS-coronavirus adaptation to human ACE2. The EMBO journal. 2005; 24(8):1634–1643. [PubMed: 15791205]

85. Wu K, Chen L, Peng G, Zhou W, Pennell CA, Mansky LM, et al. A virus-binding hot spot on human angiotensin-converting enzyme 2 is critical for binding of two different coronaviruses. Journal of virology. 2011; 85(11):5331–5337. [PubMed: 21411533]

86. Li W, Greenough TC, Moore MJ, Vasilieva N, Somasundaran M, Sullivan JL, et al. Efficient replication of severe acute respiratory syndrome coronavirus in mouse cells is limited by murine angiotensin-converting enzyme 2. Journal of virology. 2004; 78(20):11429–11433. [PubMed: 15452268]

87. Wu D, Tu C, Xin C, Xuan H, Meng Q, Liu Y, et al. Civets are equally susceptible to experimental infection by two different severe acute respiratory syndrome coronavirus isolates. Journal of virology. 2005; 79(4):2620–2625. [PubMed: 15681462]

88. Frieman M, Yount B, Agnihothram S, Page C, Donaldson E, Roberts A, et al. Molecular determinants of severe acute respiratory syndrome coronavirus pathogenesis and virulence in young and aged mouse models of human disease. Journal of virology. 2012; 86(2):884–897. [PubMed: 22072787]

89. Zornetzer GA, Frieman MB, Rosenzweig E, Korth MJ, Page C, Baric RS, et al. Transcriptomic analysis reveals a mechanism for a prefibrotic phenotype in STAT1 knockout mice during severe acute respiratory syndrome coronavirus infection. Journal of virology. 2010; 84(21):11297–11309. [PubMed: 20702617]

90. Frieman MB, Chen J, Morrison TE, Whitmore A, Funkhouser W, Ward JM, et al. SARS-CoV pathogenesis is regulated by a STAT1 dependent but a type I, II and III interferon receptor independent mechanism. PLoS pathogens. 2010; 6(4):e1000849. [PubMed: 20386712]

91. Day CW, Baric R, Cai SX, Frieman M, Kumaki Y, Morrey JD, et al. A new mouse-adapted strain of SARS-CoV as a lethal model for evaluating antiviral agents in vitro and in vivo. Virology. 2009; 395(2):210–222. [PubMed: 19853271]

92. Coleman CM, Matthews KL, Goicochea L, Frieman MB. Wild-type and innate immune-deficient mice are not susceptible to the Middle East respiratory syndrome coronavirus. The Journal of general virology. 2014; 95(Pt 2):408–412. [PubMed: 24197535]

93. de Wit E, Prescott J, Baseler L, Bushmaker T, Thomas T, Lackemeyer MG, et al. The Middle East respiratory syndrome coronavirus (MERS-CoV) does not replicate in Syrian hamsters. PloS one. 2013; 8(7):e69127. [PubMed: 23844250]

94. Raj VS, Smits SL, Provacia LB, van den Brand JM, Wiersma L, Ouwendijk WJ, et al. Adenosine deaminase acts as a natural antagonist for dipeptidyl peptidase 4-mediated entry of the Middle East respiratory syndrome coronavirus. Journal of virology. 2014; 88(3):1834–1838. [PubMed: 24257613]

95. de Wit E, Rasmussen AL, Falzarano D, Bushmaker T, Feldmann F, Brining DL, et al. Middle East respiratory syndrome coronavirus (MERS-CoV) causes transient lower respiratory tract infection

Author Manuscript Author Manuscript Author Manuscript Author Manuscript

in rhesus macaques. Proceedings of the National Academy of Sciences of the United States of America. 2013; 110(41):16598–16603. [PubMed: 24062443]

96. Falzarano D, de Wit E, Feldmann F, Rasmussen AL, Okumura A, Peng X, et al. Infection with MERS-CoV causes lethal pneumonia in the common marmoset. PLoS pathogens. 2014; 10(8):e1004250. [PubMed: 25144235]
97. Munster VJ, de Wit E, Feldmann H. Pneumonia from human coronavirus in a macaque model. The New England journal of medicine. 2013; 368(16):1560–1562. [PubMed: 23550601]
98. Yao Y, Bao L, Deng W, Xu L, Li F, Lv Q, et al. An animal model of MERS produced by infection of rhesus macaques with MERS coronavirus. The Journal of infectious diseases. 2014; 209(2): 236–242. [PubMed: 24218506]
99. Falzarano D, de Wit E, Rasmussen AL, Feldmann F, Okumura A, Scott DP, et al. Treatment with interferon-alpha2b and ribavirin improves outcome in MERS-CoV-infected rhesus macaques. Nature medicine. 2013; 19(10):1313–1317.
100. Wang N, Shi X, Jiang L, Zhang S, Wang D, Tong P, et al. Structure of MERS-CoV spike receptor-binding domain complexed with human receptor DPP4. Cell research. 2013; 23(8):986–993. [PubMed: 23835475]
101. Lu G, Hu Y, Wang Q, Qi J, Gao F, Li Y, et al. Molecular basis of binding between novel human coronavirus MERS-CoV and its receptor CD26. Nature. 2013; 500(7461):227–231. [PubMed: 23831647]
102. Barlan A, Zhao J, Sarkar MK, Li K, McCray PB Jr, Perlman S, et al. Receptor variation and susceptibility to Middle East respiratory syndrome coronavirus infection. Journal of virology. 2014; 88(9):4953–4961. [PubMed: 24554656]
103. van Doremalen N, Miazgowicz KL, Milne-Price S, Bushmaker T, Robertson S, Scott D, et al. Host species restriction of Middle East respiratory syndrome coronavirus through its receptor, dipeptidyl peptidase 4. Journal of virology. 2014; 88(16):9220–9232. [PubMed: 24899185]
104. Cockrell AS, Peck KM, Yount BL, Agnihothram SS, Scobey T, Curnes NR, et al. Mouse dipeptidyl peptidase 4 is not a functional receptor for Middle East respiratory syndrome coronavirus infection. Journal of virology. 2014; 88(9):5195–5199. [PubMed: 24574399]
105. Zhao J, Li K, Wohlford-Lenane C, Agnihothram SS, Fett C, Zhao J, et al. Rapid generation of a mouse model for Middle East respiratory syndrome. Proceedings of the National Academy of Sciences of the United States of America. 2014; 111(13):4970–4975. [PubMed: 24599590]
106. Doudna JA, Charpentier E. The new frontier of genome engineering with CRISPR-Cas9. Science. 2014; 346(6213):1258096. Genome editing. [PubMed: 25430774]
107. Zhang N, Jiang S, Du L. Current advancements and potential strategies in the development of MERS-CoV vaccines. Expert review of vaccines. 2014; 13(6):761–774. [PubMed: 24766432]
108. Chan JF, Chan KH, Kao RY, To KK, Zheng BJ, Li CP, et al. Broad-spectrum antivirals for the emerging Middle East respiratory syndrome coronavirus. The Journal of infection. 2013; 67(6): 606–616. [PubMed: 24096239]
109. Hart BJ, Dyall J, Postnikova E, Zhou H, Kindrachuk J, Johnson RF, et al. Interferon-beta and mycophenolic acid are potent inhibitors of Middle East respiratory syndrome coronavirus in cell-based assays. The Journal of general virology. 2014; 95(Pt 3):571–577. [PubMed: 24323636]
110. Coleman CM, Liu YV, Mu H, Taylor JK, Massare M, Flyer DC, et al. Purified coronavirus spike protein nanoparticles induce coronavirus neutralizing antibodies in mice. Vaccine. 2014; 32(26): 3169–3174. [PubMed: 24736006]
111. de Wilde AH, Jochmans D, Posthuma CC, Zevenhoven-Dobbe JC, van Nieuwkoop S, Bestebroer TM, et al. Screening of an FDA-approved compound library identifies four small-molecule inhibitors of Middle East respiratory syndrome coronavirus replication in cell culture. Antimicrobial agents and chemotherapy. 2014; 58(8):4875–4884. [PubMed: 24841269]
112. Dyall J, Coleman CM, Hart BJ, Venkataraman T, Holbrook MR, Kindrachuk J, et al. Repurposing of clinically developed drugs for treatment of Middle East respiratory syndrome coronavirus infection. Antimicrobial agents and chemotherapy. 2014; 58(8):4885–4893. [PubMed: 24841273]

Author Manuscript Author Manuscript Author Manuscript Author Manuscript

113. Kim E, Okada K, Kenniston T, Raj VS, AlHajri MM, Farag EA, et al. Immunogenicity of an adenoviral-based Middle East Respiratory Syndrome coronavirus vaccine in BALB/c mice. Vaccine. 2014; 32(45):5975–5982. [PubMed: 25192975]

114. Zhang N, Tang J, Lu L, Jiang S, Du L. Receptor-binding domain-based subunit vaccines against MERS-CoV. Virus research. 2014

Author Manuscript Author Manuscript Author Manuscript Author Manuscript

Highlights

- We discuss the development of animal models for SARS and MERS-CoV.
- Strategies to develop models for the FDA “Animal Rule” are illustrated.
- Host range is discussed in the context of viral receptor heterogeneity.

Author Manuscript Author Manuscript Author Manuscript Author Manuscript

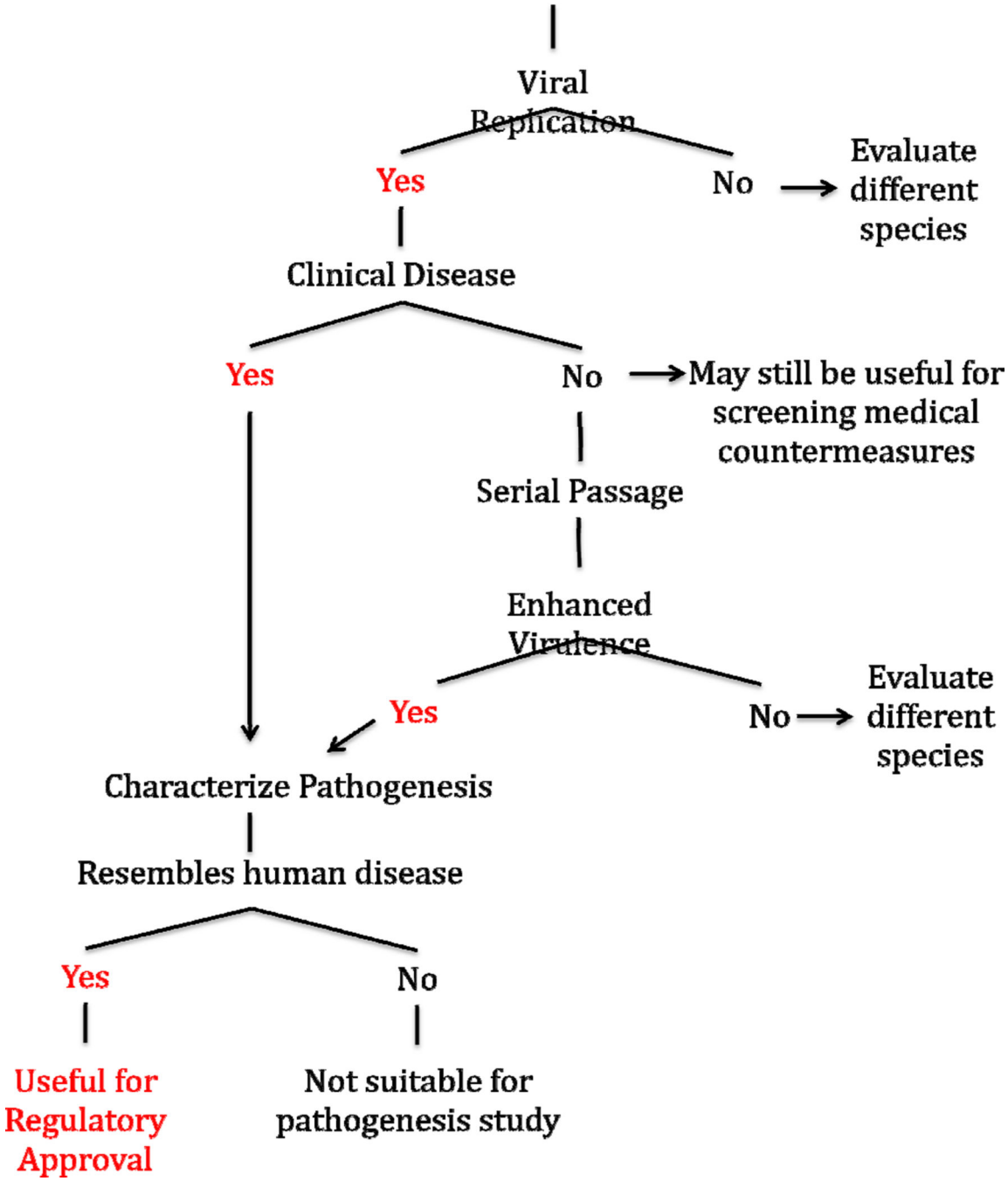

Figure 1. Schematic of strategies to develop an animal model to meet the FDA *Animal Efficacy Rule*

Under the FDA's *Animal Efficacy Rule* ("Animal Rule") therapeutics against rare, emerging, or virulent agents can achieve regulatory approval provided efficacy is demonstrated in two animal models (one of which must be a non-rodent species). Animal species of interest must first be evaluated for permissiveness to viral replication and presentation of clinical disease. As an alternative, in animal species that are permissive but do not show clinical disease, serial passage can be performed. After an animal model has been developed the resulting

Author Manuscript Author Manuscript Author Manuscript Author Manuscript

disease must be characterized. The ideal animal model is permissive to infection and reproduces the clinical illness and pathology observed in humans.

Author Manuscript Author Manuscript Author Manuscript Author Manuscript

Virology. Author manuscript; available in PMC 2016 May 01.

Table 1

ACE2 Amino acid residues from different species that interact with S proteins from SARS coronaviruses

ACE2 sequence*		**Amino Acid Positions at which sequences differ from human ACE2 sequence (human ACE2 numbering)**																	
		24	**27**	**31**	**34**	**35****	**37**	**38**	**41**	**42**	**45**	**79**	**82**	**83**	**90**	**325**	**329**	**330**	**353**	**354**
Specis	Human	Q	T	**K**	H	E	E	**D**	**Y**	Q	L	L	**M**	Y	N	Q	E	N	**K**	G
	African Green monkey																			
	Rhesus macaque																			
	Cynomolgus macaque[a]																			
	Marmoset[a]								H	E			T							
	Civet	L		T	Y		Q	E			V		T		D					
	Ferret	L			Y			E				H	T		D	E	N			R
	Rat	K	S		Q							I	N			P	T		H	
	Mouse	N		N	Q							T	S	F	T		A		H	
	Hamster[a]				Q								N							
Receptor binding site		Corresponding amino acid positions and residues of SARS-CoV spike proteins that interact with ACE2																		
S protein sequence in indicated virus	Tor2	N473	Y475	**Y475**	Y440	N479**	Y491	**Y436**	**Y484**	Y436	Y484	L472	**L472**	N473	T402	R426	R426	T486	**G488**	Y491
				Y442	N479				**T486**	Y484				Y475					**T487**	G488
									T487										**Y491**	
	MA15							Y436H		Y436H										
	v2163			Y442F				Y436H		Y436H										
	MA20			Y442L	N479K															

*Only residues that are different from human DPP4 are displayed

Sites that play an important in host range and cross species infection are indicated in bold type and are underlined

[a]Denotes predicted sequence of DPP4

**Position 35 does not directly contact the S-protein RBD but influences interactions at positions 31 and 38

Accession Numbers: Human (AB046569), African Green monkey (AY996037), Rhesus macaque (NM_001135696), Cynomolgus macaque (XM_005593037), Marmoset (XM_008988993.1), Civet (AY881174), Ferret (AB208708), Rat (NM_001012006), Mouse (NM_001130513), Hamster (XM_005074209)

Adapted from Li F, et al., 2005 Science

Author Manuscript Author Manuscript Author Manuscript Author Manuscript

Table 2

DPP4 amino acid sequences from different species predicted to interact with the MERS Spike protein.

Species	Amino Acid residues that differ from human DPP4 (human DPP4 numbering†)														
	229	**267**	**286**	**288**	**291**	***294***	***295***	***298***	***317***	**322**	**336**	**341**	***344***	**346**	**Accession no.**
Human	N	K	Q	T	A	*L*	*I*	*H*	*R*	Y	R	V	*Q*	I	NM_001935
Rhesus macaque															KF574267
Common marmoset*															XM_002749392
Camel				V											KJ002534
Mouse				P		*A*	*R*				T	S		V	NM_001159543
Hamster*					**E**		*T*				T	L		V	XM_007610182
Ferret			E		D	*S*	*T*	*Y*			S	E	*E*	T	DQ266376
Cotton			E		E	*A*	*T*				T	L		V	
Rat**															
Bat						-	*T*	-	-		K		-		KC249974

* denotes predicted sequence

** unpublished sequence generated by sequencing DPP4 from cotton rat lung tissue

† Modified from van Doremalen N et al., 2014 JV

Residues in patch 1 are underlined and residues in patch 2 are in italics and underlined.